Advanced Butler matrices with integrated bandpass filter functions

Tornielli di Crestvolant, Vittorio; Martin Iglesias, Petronilo; Lancaster, Michael

DOI:
10.1109/TMTT.2015.2460739

Advanced Butler Matrices With Integrated Bandpass Filter Functions

Vittorio Tornielli di Crestvolant, *Graduate Student Member, IEEE*, Petronilo Martin Iglesias, *Member, IEEE*, and Michael J. Lancaster, *Senior Member, IEEE*

***Abstract*—A novel class of Butler matrix with inherent bandpass filter (BPF) transfer functions is presented in this paper. The Butler matrix is the fundamental network to split and recombine the signal in multi-port power amplifiers, however, to suppress spurious frequencies generated by the amplifiers or to provide near-band rejection in order not to interfere with other transmission/receiving bands separate filtering is often required. Here, the traditional power division and phase distribution of the Butler matrix are included together with filtering selectivity into one single device based only on coupled resonators. An analytical synthesis procedure of the coupling matrix for $2^k \times 2^k$ networks is presented here for the first time. The proposed solution has shown significant advantages in terms of size reduction compared to the traditional baseline consisting of a distribution network plus a bank of BPFs. The synthesis and design of a 2×2, 180° hybrid coupler at 10 GHz and a 4×4 Butler matrix with an equal-ripple four-pole Chebyshev bandpass characteristic centred at 12.5 GHz with 500-MHz bandwidth are described, confirming the synthesis technique proposed. Two models of the 4×4, one built with additive manufacturing and the other with milling, are also presented and compared. Experimental measurements are in good agreement with both simulations and theoretical expectations.**

***Index Terms*—Bandpass filters (BPFs), Butler matrix, circuit synthesis, multi-port power amplifier (MPA), power distribution.**

I. Introduction

THE BUTLER matrix is a multiple input and multiple output network with the purpose of spreading the input signals at the output ports with prescribed power and phase distribution. In the very first studies, the Butler matrix (also known as the B matrix) was introduced as a beam-forming network (BFN) where multiple signals have to feed an array antenna [1], [2]. In its basic configuration, the Butler matrix is formed by several hybrid power dividers and phase shifters: analytical procedures have been derived in order to systematically design the antenna pattern depending on the number of beams [3]–[6]. The fundamental building block of these networks is the branch-line directional coupler, which is a 2 $\times$ 2 hybrid network where the power at one input is equally divided with a phase shift of 90° across the two outputs [7]. The physical structure of the hybrid consists of two pairs of parallel and orthogonal quarter-wave transmission lines with given characteristic impedance that equally split the input power providing a quadrature phase response [7]. Additional work to extend the operational bandwidth, or to define the arbitrary output power splitting ratio, of the hybrid has been presented in [8] and [9]. The same concept can also be achieved with the use of 180° hybrid couplers in place of the 90°, through a different design procedure [10].

Other than BFNs, the Butler matrix has found a fundamental application in multi-port power amplifiers (MPAs), with the first study of Sandrin [11]. The idea around the MPA is that the N input signals are equally distributed among N identical power amplifiers (typically traveling-wave-tube amplifiers or solid-state power amplifiers) operating in the linear region. In this case, all the amplifiers share all the signals. Later, all the signals coming from the amplifiers are reconstructed in order to avoid interference. This initial split of the input signals is performed by a Butler matrix, also called the input network (INET). The phase distribution provided by the input Butler matrix is exploited in order to, theoretically, re-obtain the same initial signals, but amplified at the output. The recombination network is cascaded to the power amplifiers and is also called the output network (ONET). In practice, the ONET is identical to the INET, except for being mirrored. In principle, one design of the Butler matrix is sufficient in order to have both the INET and ONET. From a topological point of view, it is not necessary to have any internal or external phase shifter for the $N = 2^k$ input/output Butler matrix used for an MPA [12], [13]. This is an important aspect, as it shows that the phase shift provided by the branch-line couplers of the network is sufficient for the recombination stage of the MPA. The MPA solution finds extensive applications in telecommunication satellites and multi-beam antenna configurations [14]. The main advantage of the MPA over the traditional paralleled high power amplifiers (HPAs), one per beam, is in more flexibility of the power allocation among the single amplifiers and a better absorption of traffic in case of failure of one of the HPAs if no redundancy is provided [15].

The Butler matrices proposed in the literature for MPAs are mainly implemented with several hybrid couplers based on transmission lines, producing a broadband response. If it is required to suppress the spurious frequencies or the intermodu-

Manuscript received November 25, 2014; revised May 08, 2015 and July 03, 2015; accepted July 17, 2015. This work was supported by the Networking/Partnering Initiative between the University of Birmingham, the European Space Agency, and Airbus Defence and Space under Contract 4000107492/13/NL/GLC/fe.

V. Tornielli di Crestvolant and M. J. Lancaster are with the School of Electronic, Electrical, and Systems Engineering, University of Birmingham, Birmingham B15 2TT, U.K. (e-mail: vittorio.tornielli@gmail.com; m.j.lancaster@bham.ac.uk).

P. M. Iglesias is with the European Space Agency (ESA), European Space Research and Technology Centre (ESTEC), 2200 AG Noordwijk, The Netherlands (e-mail: petronilo.martin.iglesias@esa.int).

Digital Object Identifier 10.1109/TMTT.2015.2460739

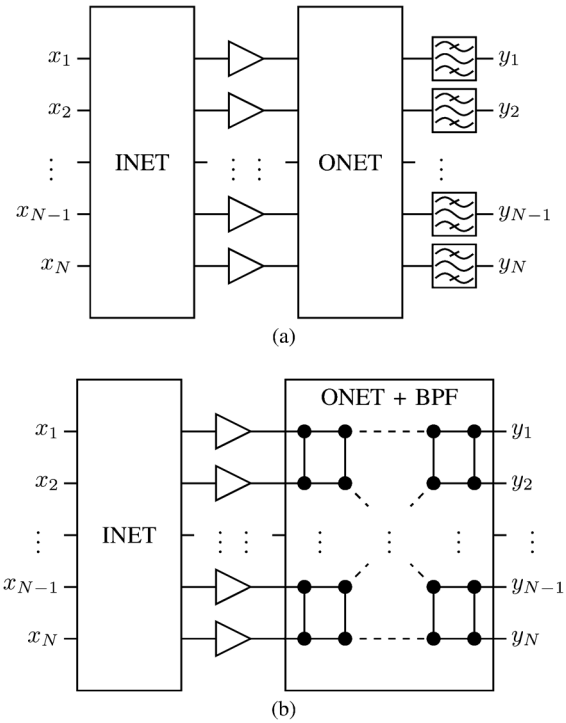

Fig. 1. Schematic of: (a) MPA with BPFs cascaded and (b) proposed network based on coupled resonators (black dots) with the ONET including all the filtering transfer functions.

lation products generated by the HPAs, separate bandpass filter (BPF) or low-pass filter (LPF) interfaces need to be cascaded to the ONET, as shown in Fig. 1(a). This configuration has been adopted in various telecommunication satellites for S- and L-band [16]. The extra filters lead to bulky equipment, which can be of critical importance, especially in satellite applications where there are stringent constraints in the size of the on-board devices.

The solution proposed in this work is to incorporate the bandpass filtering function and the Butler matrix into one single circuit based solely on coupled resonators. The new Butler matrix that includes all the filter transfer functions will substitute the ONET plus BPFs, resulting in sensible size and mass reduction. Fig. 1(b) is a representation of the MPA that includes the ONET with inherent BPFs, as it will be presented in this paper. It will be shown that the proposed solution is capable of completely eliminating the ONET of Fig. 1(a) with no redundancy in terms of number of resonant cavities. An analytical synthesis technique will also be presented for a step-by-step procedure starting from the RF specification until the final formulation of the coupling matrix. The attempt to introduce filtering functions into the 2 $\times$ 2 hybrid was already presented in [17]–[24] and a circuital diagram of a 4 $\times$ 4 matrix with the coupling coefficients calculated via optimization techniques has been introduced [21]. The four-resonator hybrid is also extensively exploited to create more complex subsystems in [25], however, optimization of the inverters are mandatory in order to obtain desired symmetries and frequency response. Also, no general understanding of the polynomials for the mentioned multi-port circuits is provided. Other structures implementing input/output power division and filtering through coupled resonators structures are discussed in [26]–[29], however, they do not provide an analytical synthesis of the coupling matrix. A different type of solution for networks with one input to multiple outputs has been presented for microstrip [30].

In this work, a general and analytical synthesis technique of the coupling matrix of $N \times N$ Butler matrices with an inherent filter function (Chebyshev or Butterworth) based on resonators is introduced. The synthesis is for any $2^k \times 2^k$ reciprocal 180° Butler matrix. One prototype of a 2 $\times$ 2 hybrid and two breadboards of a 4 $\times$ 4 Butler matrix made with additive manufacturing and milling are presented, showing that current synthesis successfully adapts to new, as well as known, technologies. The RF measurements compared to the theoretical curves, show good match, and confirm the analytical description.

II. General Considerations

A. Network Assumptions

In stable conditions the MPA behaves simply as a bank of power amplifiers in parallel, and theoretically, there is no distortion derived from the INET or ONET. The concept can be expressed in term of transfer function matrices as

$$[\boldsymbol{T}_{\mathrm{MPA}}] = [\boldsymbol{T}_{\mathrm{INET}}] \cdot G[\boldsymbol{I}_N] \cdot [\boldsymbol{T}_{\mathrm{ONET}}] \tag{1}$$

where all the amplifiers produce the same gain G and $[I_N]$ is the $N \times N$ unitary matrix. The transfer function matrix of the whole MPA is indicated with $\boldsymbol{T}_{\mathrm{MPA}}$ while the ones for the INET and ONET with, respectively, $\boldsymbol{T}_{\mathrm{INET}}$ and $\boldsymbol{T}_{\mathrm{ONET}}$. The cascade of INET and ONET should be transparent to the system, meaning that (1) should result, except for the scaling factor G, in a unitary matrix or any of its transposition. This is because a signal entering at input x_1 of Fig. 1 can reach any of the outputs if there is no mutual interference. In general, it is possible to say that (1) should result in a *permutation* matrix. The Butler matrix based on 90° hybrid directional couplers, for example, produces a transfer function matrix that is, apart for an amplitude and phase scaling factor, an anti-diagonal unitary matrix, as shown with closed formulas in [12].

Here, the new Butler matrix with filtering included is obtained through a synthesis technique of a multi-port circuit based on coupled resonators, as shown in the general schematic of Fig. 1(b). Thus, it is convenient to express the electrical properties of a lossless network formed of p ports and n resonators through a coupling matrix defined by blocks, as introduced in [31]

$$\boldsymbol{M} = \begin{bmatrix} \boldsymbol{M_p} & \boldsymbol{M_{pn}} \\ \boldsymbol{M_{np}} & \boldsymbol{M_n} \end{bmatrix} \tag{2}$$

where

- $\boldsymbol{M_p} \in \mathbb{R}^{p \times p}$ is the matrix of the coupling coefficients between external ports;
- $\boldsymbol{M_{pn}} \in \mathbb{R}^{p \times n}$ is the matrix of the coupling coefficients between resonators external ports ($\boldsymbol{M_{np}} = \boldsymbol{M_{pn}^T}$);
- $\boldsymbol{M_n} \in \mathbb{R}^{n \times n}$ is the matrix of the coupling coefficients between internal resonators.

$\boldsymbol{M}$ is a square matrix of dimensions $p + n$.

In recent years, there has been increasing interest in the general synthesis of multi-port networks based on coupled resonators [32]–[35]. However, many limitations of fully direct

analytical synthesis methods have been faced, both in the definition of the polynomials of networks with more than three ports and with the maximum number of couplings that each resonator can sustain [36]. Modern techniques to synthesize multi-port circuits, once the constituting rational polynomials are known, comprise the synthesis of an equivalent transversal network and later apply a sequence of matrix similarities (matrix rotations) in order to obtain the final topology [31], [37]. This process is based on the conversion between the rational form of the scattering polynomials to the admittance matrix parameters $[\boldsymbol{Y}]_{ij}$ expressed as ratio between numerators n_{ij} and a common denominator y_d as in the following partial fraction expansion notation:

$$[\boldsymbol{Y}]_{ij} = \frac{n_{ij}}{y_d} = [\boldsymbol{Y}^{\boldsymbol{\infty}}]_{ij} + \sum_{h=1}^{n} \frac{r_{ij,h}}{s - \mathrm{j}\lambda_h} \tag{3}$$

where $[\boldsymbol{Y}^{\boldsymbol{\infty}}]_{ij}$ is the limit at infinity of the generic element of the admittance matrix, $r_{ij,h}$ is the residue associated with pole λ_h, the complex low-pass frequency is $s = \sigma + \mathrm{j}\omega$, and n is the order of the polynomial of the common denominator y_d. From (3), direct expressions of the elements of matrices $\boldsymbol{M_p}$, $\boldsymbol{M_n}$, and $\boldsymbol{M_{pn}}$ can be obtained [38]. The conversion between the different types of matrices can be performed either analytically for some simple cases [35] or through numerical methods [39]. However, these techniques proved their validity mainly for multiplexing applications, and in particular when the transfer function exhibits all single poles [35]. If the last condition is not met, the method based on the derivation of the equivalent transversal network cannot be used. For the Butler matrix, all the signals are operating inside an available spectra of the same operational bandwidth, and center frequency with the input ports mutually isolated. This brings singularities to the transversal network coupling matrix, leading to a reduction of its columns/rows, and thus to the elimination of some ports/resonators.

The solution proposed in [25] provides an interesting combination of many 2×2 hybrids to create multi-port networks. Analytical formulas are presented for the basic hybrid, but they are not easily scalable to a higher number of ports due to the intrinsic limitations of the even/odd mode technique. Moreover, the synthesis of the inverters and resonators are performed through an equivalence with the Chebyshev filtering characteristic. Due to these problems, the polynomials for the proposed multi-port networks are not provided, a different approach is presented here.

In addition, the topology of the network is yet to be defined. Hence, the requirements and assumptions of the resonator-based Butler matrix can be summarized as follows:

1) mutually isolated input ports;
2) equal input power distribution among the outputs;
3) appropriate input to output phase distribution in order to grant recombination of the signals;
4) reciprocal network;
5) same bandpass transfer function for all signals.

In order to satisfy the condition of same transfer function, it follows that is not possible to exploit (3) because of the higher multiplicity of roots of common denominator y_d, hence, a different method shall be investigated.

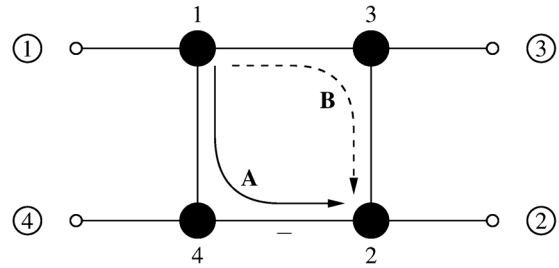

Fig. 2. Schematic of a 180° hybrid coupler based on coupled resonators.

In the following, a general method is proposed for the synthesis of any $N \times N$ Butler matrix with filter transfer functions included exploiting the virtual open circuit offered by the 180° hybrid coupler based on resonators [19], hence, avoiding the problem of multiplicity of roots of y_d that affects traditional techniques.

B. Virtual Open Circuit

Fig. 2 shows the schematic of a 180° hybrid coupler based on coupled resonators. Black circles are resonators with the electromagnetic (EM) couplings represented here by lines. The network shows the response of a typical rat-race coupler with a two-pole filtering characteristic [19], where the coupling matrix is defined as

$$\boldsymbol{M_p} = \boldsymbol{0} \tag{4a}$$

$$\boldsymbol{M_{pn}} = K_e \boldsymbol{I}_4 \tag{4b}$$

$$\boldsymbol{M_n} = \begin{bmatrix} 0 & 0 & K_u & K_u \\ 0 & 0 & K_u & -K_u \\ K_u & K_u & 0 & 0 \\ K_u & -K_u & 0 & 0 \end{bmatrix}. \tag{4c}$$

It can be shown that parameters K_e and K_u are directly related to the external and internal couplings of a two-pole filter with a scaling of a factor $1/\sqrt{2}$ for the latter [17], [19]. If a source is applied to port 1, the signal propagates to ports 2 through paths A and B shown in Fig. 2. All the coupling coefficients are the same, except for the one between resonators 2 and 4, which is same magnitude, but negative. In resonator 2 there exits a totally destructive combination of signals from paths A and B that generate the perfect isolation at port 2. This provides a virtual open circuit at resonator 2 when considering paths from ports 1 to 3 and from 1 to 4. The same is valid for pairs of any other opposite ports. It should be noted that the network exhibits two identical filter functions, with two poles each, while the network has four resonators. The topology shown in Fig. 2 will be adopted in the next sections as the fundamental building block of a generalized $N \times N$ Butler matrix.

C. Transfer Function Requirements

The electrical properties of the four-resonator 180° coupler of Fig. 2 are exploited in order to make the synthesis of a general $N \times N$ Butler matrix with $N = 2^k$. The transfer function matrix, defined over the operational bandwidth, of the hybrid is the typical one of a rat-race coupler

$$\boldsymbol{T}_{180^\circ} = \boldsymbol{T}_1 = \frac{1}{\sqrt{2}} \begin{bmatrix} 1 & 1 \\ 1 & -1 \end{bmatrix}. \tag{5}$$

Here input signals are applied to ports 1 and 2 of Fig. 2, and outputs are at ports 3 and 4. By recursive combination of (5), a Butler matrix can be obtained in a similar fashion to that described in [12] using only 180° hybrid couplers. The total transfer matrix defined by the Kronecker product is

$$\boldsymbol{T}_k = \boldsymbol{T}_1 \otimes \boldsymbol{T}_{k-1} = \frac{1}{\sqrt{2}} \begin{bmatrix} \boldsymbol{T}_{k-1} & \boldsymbol{T}_{k-1} \\ \boldsymbol{T}_{k-1} & -\boldsymbol{T}_{k-1} \end{bmatrix}. \tag{6}$$

This is also known as the Hadamard matrix. Naturally, the Hadamard matrix is orthogonal, indeed becoming very attractive for the architecture of Fig. 1. It is possible to assign to the INET a Butler matrix with a transfer function like the one of (6), and to the ONET, the same network, but mirrored. The mirroring of the input/output of the ONET corresponds to the transposition of the transfer function matrix. Recalling (1) and the orthogonality of the Hadamard matrix it can be shown how this kind of network is suitable for the use in MPAs in the operational bandwidth. Combining (6) with (1) the following is derived:

$$\begin{bmatrix} y_1 \\ y_2 \\ \vdots \\ y_N \end{bmatrix} = [\boldsymbol{T}_k] \cdot G[\boldsymbol{I}_N] \cdot [\boldsymbol{T}_k]^T \begin{bmatrix} x_1 \\ x_2 \\ \vdots \\ x_N \end{bmatrix} = G \begin{bmatrix} x_1 \\ x_2 \\ \vdots \\ x_N \end{bmatrix}. \tag{7}$$

This states that using a combination of 180° hybrid coupler, the transfer function of the entire MPA results in a multiplication of the amplitude of the input signals of a factor G.

III. Synthesis Technique

A. Polynomials Definitions

The network has $2N$ ports (i.e., inputs $1, \ldots, N$ and outputs $N+1, \ldots, 2N$), it is reciprocal, lossless, is described by its $\boldsymbol{S}$ scattering matrix and has the generic transfer function matrix $\boldsymbol{T}_k$ defined in (6). The reflection (α), transmission (β), and isolation (γ) parameters are directly related with the $\boldsymbol{S}$ elements with the following simplified notation:

$$\alpha_r = S_{r,r}, \qquad \text{for } r \leq N \tag{8a}$$
$$\beta_i = S_{r,i+N}, \qquad \text{for } i \leq N \tag{8b}$$
$$\gamma_j = S_{rj}, \qquad \text{for } 1 < j \leq N; \quad \wedge\, r \neq j \tag{8c}$$

where α_r is the reflection characteristic seen at port r, β_i is the transfer function between ports r and $N+i$, and γ_j is the isolation between ports r and j (with $j < N$). In (8), the input signals are assumed to be applied at one port in the range 1 to N, though the same concept is valid if the source is applied at ports $N+1$ to $2N$ due to the reciprocity of the network. For a generic lossless network, the unitary condition is expressed by the well-known formula

$$\boldsymbol{S} \cdot \boldsymbol{S}^* = \boldsymbol{I} \tag{9}$$

where $\boldsymbol{S}^*$ is the complex conjugate of matrix $\boldsymbol{S}$ and $\boldsymbol{I}$ is the identity. The set of definitions (8) can be substituted in (9), producing the following relation in terms of parameters α_r, β_i, and γ_j valid for $r \leq N$:

$$|\alpha_r|^2 + \sum_{i=1}^{N} |\beta_i|^2 + \sum_{\substack{j=1 \\ j \neq r}}^{N} |\gamma_j|^2 = 1. \tag{10}$$

The traditional cascading of a Butler matrix and a bank of BPFs, as was shown in Fig. 1(a), is taken as the reference model with scattering matrix $\boldsymbol{S}_{\text{ref}}$. It can also be studied as a reciprocal lossless network with a scattering matrix derived by the combination of the ONET and filters

$$\boldsymbol{S}_{\text{ref}} = \boldsymbol{S}_{\text{ONET}} \cdot \text{diag}\{\boldsymbol{S}_{\text{BPF}}\} \tag{11}$$

that must comply with condition (9). In this study, the nonlinearities of the ONET are not taken into account and the network is just considered as an equal power divider, except for the output phase contribution with perfect isolation between pair of input ports. With this in mind, the unitary condition (11) is applied to (9), resulting in

$$\sum_{h=1}^{N} \frac{1}{N} \left(|\alpha_{\text{BPF},h}|^2 + |\beta_{\text{BPF},h}|^2 \right) = 1 \tag{12}$$

where the return loss and transmission of the generic BPF on the output port h are indicated with parameters $\alpha_{\text{BPF},h}$ and $\beta_{\text{BPF},h}$, respectively. As the Butler matrix performs an equal power splitting, there is a term $1/N$ in (12). The assumptions made in the previous sections stated that all the inputs/outputs of the distribution network were mutually isolated and the same BPF transfer function were applied to all the ports. They are expressed in the notation introduced here with the following set of equations:

$$\sum_{i=1}^{N} |\beta_i|^2 = N|\beta|^2 \tag{13a}$$
$$\sum_{\substack{j=1 \\ j \neq r}}^{N} |\gamma_j|^2 = 0 \tag{13b}$$
$$\sum_{h=1}^{N} \frac{1}{N} |\alpha_{\text{BPF},h}|^2 = |\alpha_{\text{BPF}}|^2 \tag{13c}$$
$$\sum_{h=1}^{N} \frac{1}{N} |\beta_{\text{BPF},h}|^2 = |\beta_{\text{BPF}}|^2. \tag{13d}$$

A direct consequence of (13) is that all the insertion loss characteristics are the same, indeed, $\alpha_r = \alpha$. The unitary condition is exploited in order to equate relations (10) and (12) with the set of conditions expressed in (13),

$$|\alpha|^2 + N|\beta|^2 = |\alpha_{\text{BPF}}|^2 + |\beta_{\text{BPF}}|^2 = 1. \tag{14}$$

The two parts of (14) demonstrate the direct relation between the characteristics of the transfer functions of the circuit under investigation and the ones of a generic BPF,

$$|\alpha|^2 = |\alpha_{\text{BPF}}|^2 \tag{15}$$

$$|\beta|^2 = \frac{|\beta_{\mathrm{BPF}}|^2}{N}. \tag{16}$$

This highly simplifies the complexity of the synthesis of polynomials of the multi-port network with regard to the difficulties mentioned at the beginning of the section. The concept of the virtual open circuit used to make two independent paths in the 180° of Fig. 2 is generalized here to the case of N ports. This is a fundamental assumption to specify independent paths, each of them producing a filter transfer function. Hence, the synthesis of the generic set of functions α and β starts from that of a two-port BPF with known α_{BPF} and β_{BPF}.

B. Topology

The 180° hybrid of Fig. 2 is identified to be the suitable candidate as the fundamental building block of the Butler matrix with filtering because of the properties of perfect isolation, equal power division, and transfer function matrix compliant with the application requirements. Each independent path, needed to perform the transfer functions α and β, is obtained through a sequence of hybrid couplers of the type of Fig. 2. As each hybrid equally splits the power at the two output-transmission ports, for a single path the following number of hybrids are necessary:

$$k = \log_2 N. \tag{17}$$

The contribution of each of them to one single path is of exactly two resonators, indeed, the total transfer function achievable with the current technique produces a minimum number of poles ρ given as

$$\rho = 2k. \tag{18}$$

Moreover, each unit (i.e., 180° hybrid coupler) accepts two input signals, and hence, a number of $N/2$ units, in order to receive all the input signals, are necessary. Indeed, the entire network can be thought of as a matrix of units of $N/2$ rows and k columns with a total number u of hybrids and n resonators given by the following relations:

$$u = \frac{N}{2}k = \frac{N}{2}\log_2 N \tag{19}$$

$$n = 4u = 2N\log_2 N. \tag{20}$$

Every hybrid coupler constituting the network should be connected to other hybrids or to the external ports in order to comply with the prescribed output power and phase distribution. The structures shown in Fig. 3 solves this problem for different numbers of inputs [12]. In this figure, the input ports are indicated with $p_1, \ldots, p_N$ and the output with $q_1, \ldots, q_N$. The basic building block of the circuit is the 180° hybrid of Fig. 2. Each unit is represented with the two input ports on the left of the block, while on the right are the outputs: these are shown in Fig. 2, with ports 1, 2 for the inputs and 3, 4 for the outputs. The entire circuit described here is based on resonant cavities coupled by EM couplings, thus each line of Fig. 3 represents a coupling between pairs of resonators, which are embedded in the units shown as rectangular blocks. The figure includes the configurations of 2 × 2 [see Fig. 3(a)], 4 × 4 [see Fig. 3(b)], and 8 × 8 [see Fig. 3(c)] Butler matrices that implement the Hadamard transfer function matrix (6). It should

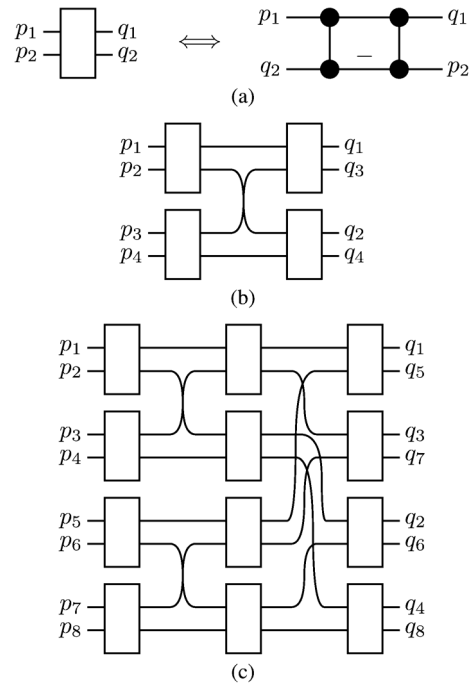

Fig. 3. Configurations of the hybrid couplers as introduced in [12], but with the lines representing EM couplings. (a) Schematic of the 2 × 2 fundamental unit and then (b) the configurations of the 4 × 4 and (c) the 8 × 8.

be noted that the numbering of the output ports q_i has been derived in the figure in order to have the phase distribution identical to the transfer function matrix of (6). However, it can be proven that if a sequential numbering, for instance, from top to bottom, is applied to the networks of Fig. 3, the resulting matrix is still orthogonal. Starting from the schematics depicted in Fig. 3, it is also possible to generalize to $N \times N$ networks recursively.

In some practical cases it might be more appropriate to change, for example, the relation between the input/output ports of some units of Fig. 3 with the ones of the 180° hybrid of Fig. 2. The reason for this change depends on particular constraints that can arise at the design stage of the single unit hybrids for specific technologies, which might lead to impractical or even impossible implementations or accommodation of the components on the circuit. The output power division of the whole Butler matrix is not affected with the change applying only to the distribution of the output phases. This, in general, is not a limit as long as the transfer function matrix is capable of recombining the signals as introduced with the general relation (1). This statement confers a greater degree of freedom to the topology configuration of the network because it does not bound the response to the only pure Hadamard transfer matrix, but gives the designer the ability to change the physical connections of the hybrids without losing the properties of the circuit.

C. Formulation of the Coupling Matrix

The synthesis technique for the formulation of the coupling matrix is summarized here with the following step-by-step procedure.

1) Review of the RF specifications. The number of input/output ports N depends on the number of signals that are

supposed to be applied to the network while the bandwidth B and the return loss RL are functions of the rejection required after the bank of power amplifiers.

2) Calculate the total number of poles ρ through (17) and (18), number of unit-hybrids u with (19), and total resonators n with (20).
3) The polynomials of the transfer function of this network are directly related to the ones of BPFs with the relations (15) and (16). This calculation is performed initially with the normalized low-pass parameters on a filter of $2k$ resonators and $2k+1$ ideal inverters. For maximally flat or equal ripple transfer functions, the low-pass g parameters are calculated with the well-known formulas [40]. The coupling coefficients of the BPF are directly obtained from g parameters with the formula

$$M_{h,\mathrm{BPF}} = \frac{1}{\sqrt{g_h g_{h+1}}} \tag{21}$$

with $h \in \{0, \ldots, 2k\}$. In order to simplify the following computations, the entity $M_{h,\mathrm{BPF}}$ is not considered here as a matrix, but just as a vector where each element represents the coupling coefficient between a pair of adjacent resonators. Alternately to the formulations of the g parameters, more advanced techniques to generate the $M_{h,\mathrm{BPF}}$ can be used as described in [41].
4) The first resonators of every 180° hybrid coupler on the first column of unit-hybrids of the circuit are all coupled with the external inputs. The same is for the second resonators of all the hybrids on the last columns that are coupled with the external outputs. The value for these coefficients correspond to the first and the last element of vector $M_{h,\mathrm{BPF}}$.
5) Each independent path has the coupling coefficients equal to the ones calculated with (21). The power splitting factor and the phase distribution are governed by the configuration of the hybrids. The hybrid's coupling coefficient K_{u_i} are all the same, except the one that is opposite phase (i.e., Fig. 2). Their magnitudes are defined as

$$K_{u_i} = \frac{1}{\sqrt{2}} M_{2i,\mathrm{BPF}} \tag{22}$$

where the subscript u_i is used to indicate all the identical hybrids on columns i. The coupling coefficients between pair of hybrids, indicated as $K_{u_i,u_{i+1}}$, are directly obtained [cf. (4b) and (4c)] as

$$K_{u_i,u_{i+1}} = M_{2i+1,\mathrm{BPF}}. \tag{23}$$

6) The coupling matrices $\boldsymbol{M_{pn}}$ and $\boldsymbol{M_n}$ are populated with the values of vectors (22) and (23) in order to reflect the chosen topology connections. Typically, $\boldsymbol{M_{pn}}$ has the values of the first and last elements of (21) for the coupling coefficients between the terminal resonators and external interfaces. The final coupling matrix of the overall network is defined by blocks with the form (2).
7) The obtained coupling matrix should be de-normalized to the center frequency f_0 and bandwidth B and expressed in term of the external quality factors Q_{em} between the external port e and the internal resonator m and the coupling coefficient k_{ij} between two internal resonators i and j as follows [41]:

$$Q_{em} = \frac{f_0}{B} \frac{1}{[\boldsymbol{M_{pn}}]^2_{em}} \tag{24a}$$

$$k_{ij} = \frac{B}{f_0} [\boldsymbol{M_n}]_{ij}. \tag{24b}$$

Note that the achievable operational bandwidth B depends on the technology of the resonator/coupling used in the physical implementation.

D. Extension of the Filtering Characteristic

The selectivity of the filtering transfer function is directly related to the number of ports N, and consequently, to the number of hybrids that produce a minimum of $\rho = 2k$ poles for every transmission parameter. However, in some cases it is required to increase the order of the network to meet the specifications. The virtual open circuit of the 180° hybrids guarantees the perfect isolation between the input ports, hence, additional resonators can be added to the ports without loss of generality given by relations (15) and (16).

For example, in a symmetric circuit the same number of resonators should be included at all output and input ports. The new transfer function will be formed by a total number of poles ρ as

$$\rho = 2k + 2v \tag{25}$$

where v is the number of resonators applied at each input and output port. The same equations for the calculation of the g parameters are used, taking into account the total number of resonators. In this case, parameters $g_1, \ldots, g_v$ and $g_{v+2k+1}, \ldots, g_{2v+2k+1}$ will apply to couplings of the resonators external to the hybrid networks, while $g_{v+1}, \ldots, g_{v+2k}$ are the ones used internally. The elements of (21) change accordingly. In this scenario, (20) is rewritten in order to take into account the extra resonators

$$n = 2N(\log_2 N + v). \tag{26}$$

The equations of the coupling coefficients internal to the hybrids (22) and of the coefficients connecting pairs of hybrids (23) remain the same, except for a shift of v positions of the elements in vector (21). Note that the generality introduced by the polynomials (15) and (16) does not limit the extension of the filtering characteristic to symmetric responses: a more complex configuration is also allowed with the possibility to provide, for example, real and/or imaginary positioned transmission zeros by means of cross couplings.

An example of response of an 8×8 symmetric Butler matrix with integrated filter function with the inclusion of the $v = 1$ resonator at each port is shown in Fig. 4. The topology of this network is the one of Fig. 3(c) with one resonator added at each input and output port. The plot shows the response in terms of reflection α and transmission β of an 8×8 Butler matrix with one extra resonator at each port and 20-dB return loss. There are eight poles in accordance with (25) and the total number of resonators required is $n = 64$. The values of the couplings coefficients in the low-pass domain are $M_{0,\mathrm{BPF}} = 0.9907$ (external coupling), $M_{1,\mathrm{BPF}} = 0.8222$ (extra resonator), $K_{u_1} =$

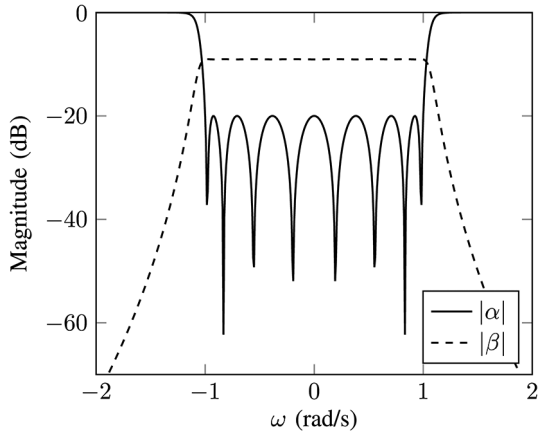

Fig. 4. Magnitude response of reflection (α) and transmission (β) of an 8 × 8 Butler matrix with $v = 1$ extra resonator at each port.

0.4183, $K_{u_2} = 0.3860$, $K_{u_3} = 0.4183$, $K_{u_1,u_2} = 0.5537$, and $K_{u_2,u_3} = 0.5537$. The physical implementation depends on the technology of resonator used.

IV. Size Reduction

Consider an $N \times N$ traditional Butler matrix formed by 90° or 180° branch line couplers with cascaded are N BPFs of $2k$ poles each (one filter per output). A total of $2kN$ cavities are necessary to obtain the required selectivity. The advanced Butler matrix proposed here incorporates both the distribution/power divider network and the filtering selectivity. These properties are achieved through a circuit based only on coupled resonators, which, without any external additional resonator, produces a filter function of $2k$ poles per output with a total number of resonant cavities equal to (20). The same performance in terms of selectivity and power distribution are obtained by the proposed Butler matrix, making redundant the ONET based on transmission lines. The saving is the space occupied by the distribution network.

The architecture of the MPA of Fig. 1(a) can be modified with the proposed solution substituting the ONET cascaded by N BPFs. This leads to a more compact configuration like the one shown in Fig. 5(a) with four inputs/outputs. The example shown in Fig. 5(b) has been synthesized for a conventional 4 × 4 ONET with the baseline of a transmission-line Butler matrix and four BPFs of the fourth order. The specification considered is $f_0 = 12.5$ GHz, a bandwidth of 500 MHz, and filters with return loss better than 25 dB. The circuit has been simulated in standard WR75 waveguide. If no isolators are considered between the Butler matrix and filter sections, the overall volume of the circuit shown in Fig. 5(b) is 96.7 cm^3. In the following it will be shown that the proposed solution of incorporating the distribution network and filters in a single components leads to a save in volume of more than 30%.

V. Prerequisite Input Signals for MPA

When operating with multiple input signals simultaneously, before port 2 of each input hybrid it is necessary to include a 90° phase shifter to avoid destruction of signals in the resonators [42]. This is needed, for example, when the Butler matrix is used in an MPA as multiple input signals are applied at the same time. The scattering parameters are obtained by measuring the ratio

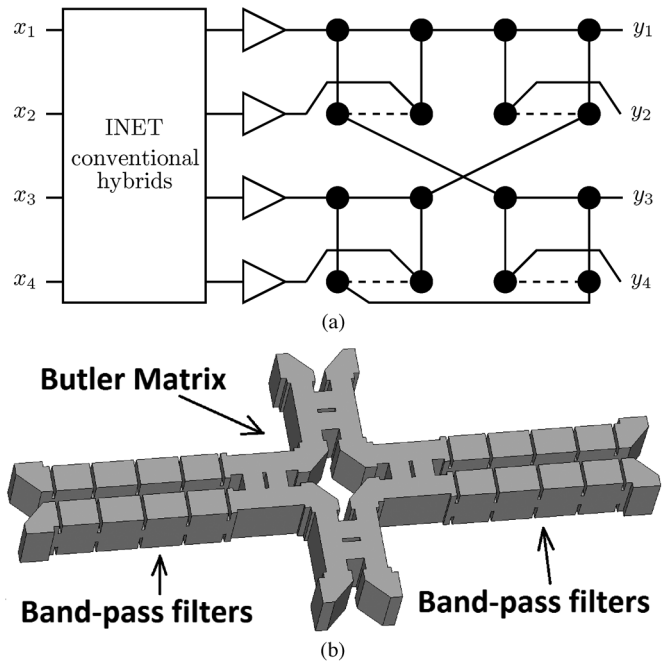

Fig. 5. Example of 4 × 4 MPA. (a) Proposed ONET including the filter functions through a circuit based on coupled resonators and (b) conventional baseline of the ONET with four BPFs cascaded to the transmission-line Butler matrix.

of the incident/reflecting waves at two ports while the others are closed on matched loads. They do not give information on the output phase distribution when multiple inputs are applied simultaneously at more ports. The Butler matrix with filtering is made here with several 180° hybrids, each of them producing out-of-phase contributions that might destroy part of the input signals. Hence, it is mandatory to keep all the fields orthogonal inside the cavities of every hybrid [42]. The phenomena is intrinsic to the nature of the 180° hybrid, and once corrected, does not affect the overall response of the MPA. This is a prerequisite for input signals that can also be operated at system level as it does not affect the configuration of the network proposed.

VI. Example Implementations

A. Compact Rat-Race 2 × 2 Hybrid Power Splitter

A 2 × 2, 180° hybrid coupler based on resonators has been implemented in standard WR90 rectangular waveguide and is shown in Fig. 6(a). The specifications to meet for this device are central frequency $f_0 = 10$ GHz, bandwidth $B = 140$ MHz, and return loss better than 25 dB. It is the physical implementation of the topology of Fig. 2, which incorporates the power division and output phase distribution of a rat-race coupler and a two-pole Chebyshev filter. This model, similar to [23], has been designed with four resonators mutually coupled by inductive irises for easy manufacturing and enhanced power-handling capabilities. The negative coupling of Fig. 2 is created by one TE_{102} cavity together with three TE_{101} cavities [43]. In this case, the synthesis of the coupling matrix reduces to the simple relations of [19] resulting, using (24), in $Q_e = 34.871$ and $k_u = 0.02145$. These values are used to obtained initial dimensions for the 3-D simulator, later optimized in order to improve the overall response [41]. With reference to the schematic of Fig. 6(b), the dimensions in millimeters are $a_1 = 23.3214$,

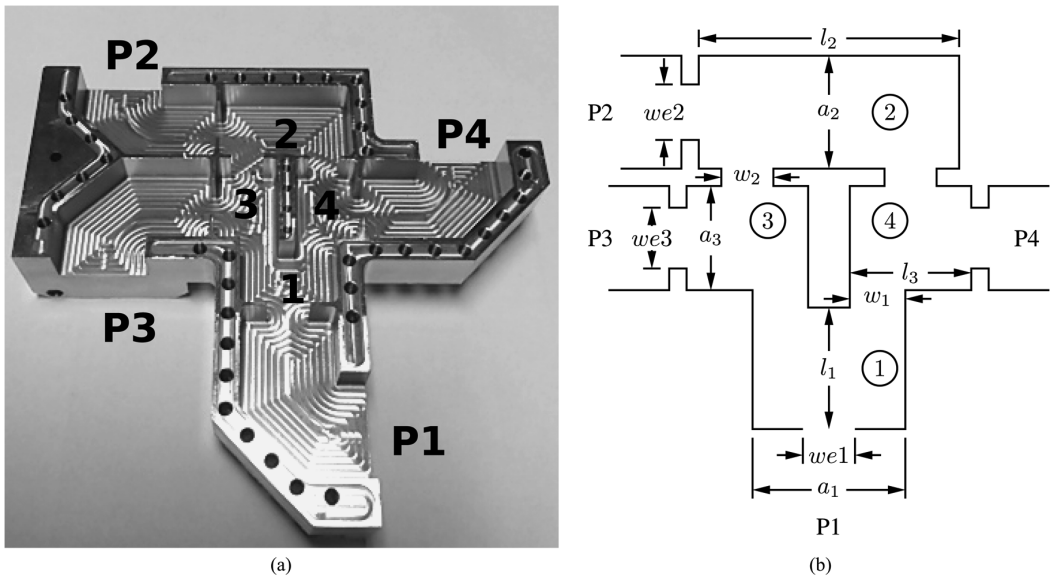

(a) (b)

Fig. 6. Rat-race 2 × 2 hybrid coupler based on resonant cavities with inductive couplings (a). Photograph of the device with ports and (b) resonators numbering and top view schematic. Four mitered bends to accommodate external flanges have been added to the final 3-D model.

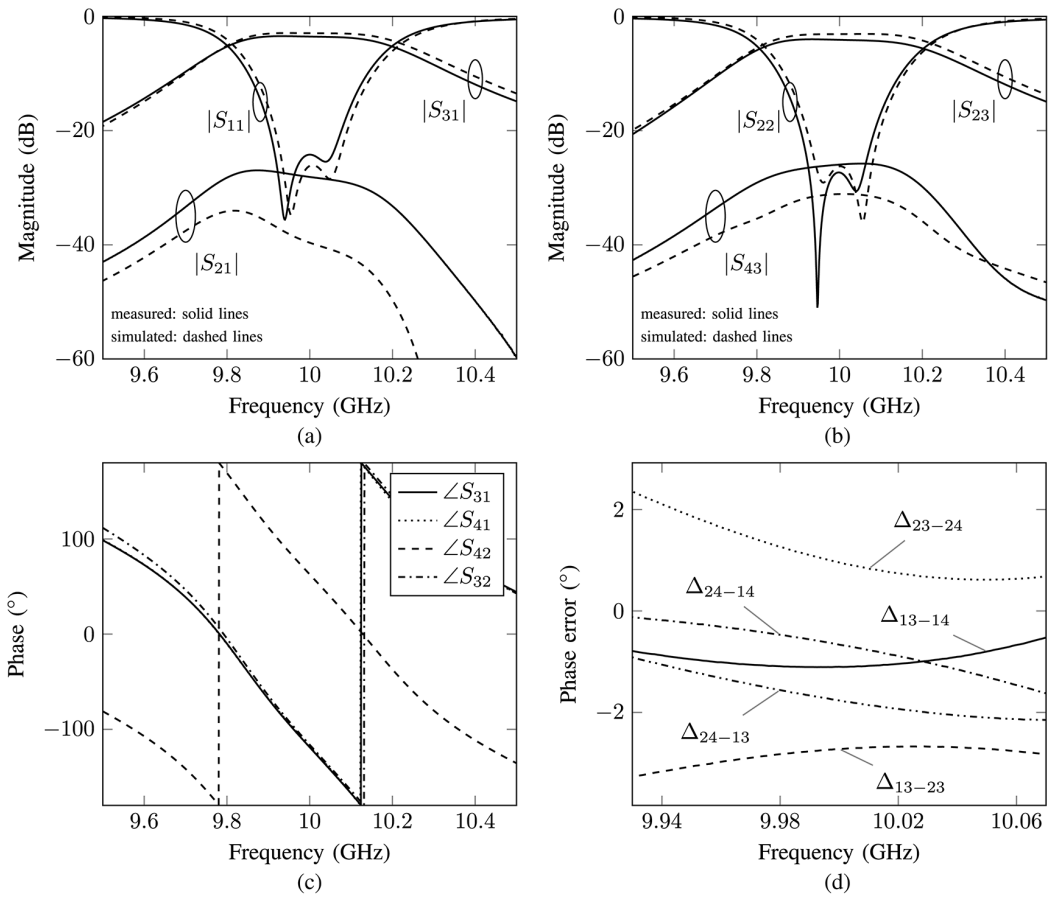

Fig. 7. Four-port 180° hybrid. Measured data (solid lines) compared to simulations (dotted lines) for the 2 × 2 hybrid coupler. (a) S_{11}, S_{21}, S_{31}. (b) S_{22}, S_{23}, S_{43}. (c) Measured output phase and (d) error of the output phase difference with respect the theoretical value.

$l_3 = 16.4116$, $w_{e1} = 10.2655$, $l_1 = 16.2032$, $w_1 = 9.6519$, $w_2 = 8.3276$, $w_{e3} = 10.3462$, $w_{e2} = 11.7542$, $l_2 = 35.2386$, and $a_2 = a_3 = 22.86$ and the thickness of iris walls is 1 mm. In the proposed case, cavity 2 introduces an asymmetry with respect to the other resonators and also with external ports. This brings the need to correct the phase of S_{32} by changing the length of the waveguide to the external port. In this example it is necessary to increase the length of the external waveguide of port 1 by a factor $\delta = 0.8$ mm with respect to the other ports.

The comparison between measured data and simulations are ploted in Fig. 7. In Fig. 7(a), the input signal is applied to port 1, while in Fig. 7(b), it is input port to 2. The hybrid has been manufactured with milling, resulting in rounded corners at the internal edges of 1.5-mm radius and with machining tolerances

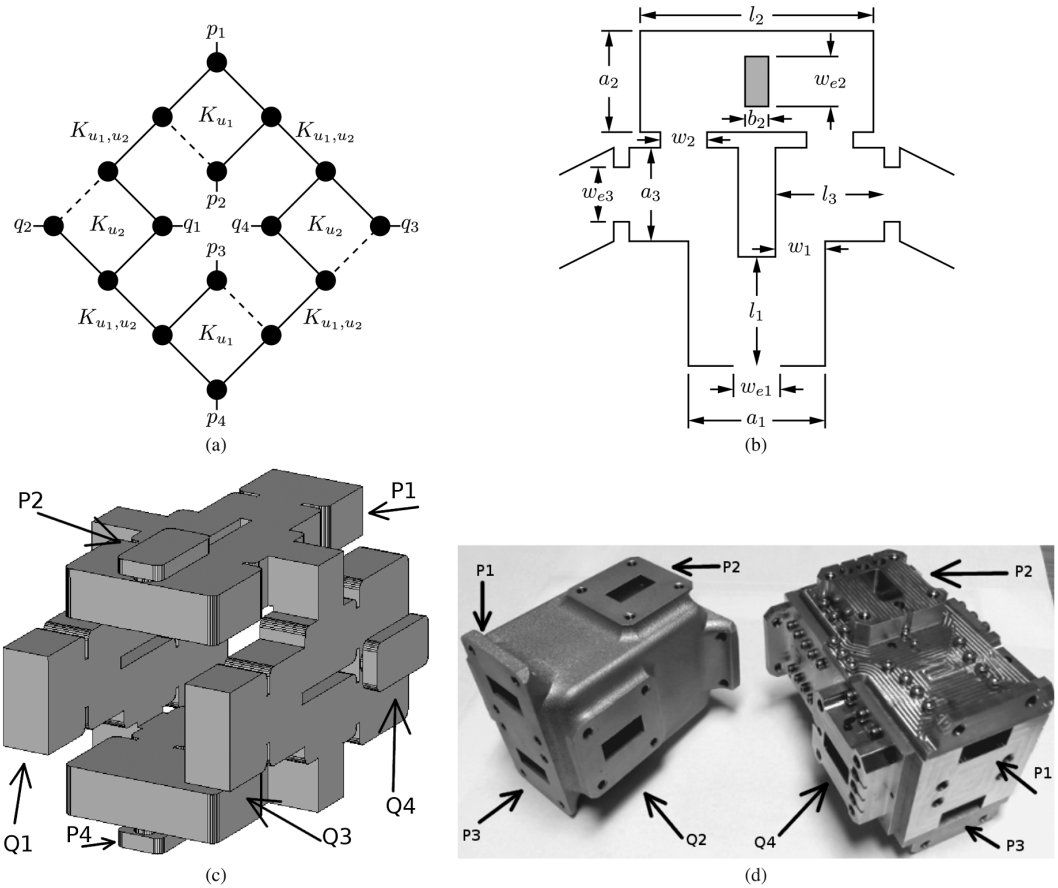

Fig. 8. (a) Topology, (b) schematic of the unit hybrid, (c) 3-D model, and (d) physical realization of the 4 × 4 Butler matrix with filtering with additive manufacturing (*left*) and milling (*right*).

of about ±20 μm with respect to the nominal value. Experimental results (solid lines) are in agreement with the simulations (dotted lines) with return loss better than 22 dB in the worst case and the isolation below 25.8 dB. The input/output phase distribution reflects of the sign elements of the transfer function matrix (5), being $\angle S_{13}$, $\angle S_{14}$, and $\angle S_{23}$ in phase and $\angle S_{24}$ out of phase, as shown in Fig. 7(c). The phase response is that of a two-pole Chebyshev filter. The in-band stability of the measured phase input–output transfer parameters is evaluated with respect to the nominal value and is shown in Fig. 7(d). The notation Δ_{ab-cd} is to indicate the error of the difference of phase responses $\angle S_{ab} - \angle S_{cd}$ with respect to the theoretical value. Over the operational bandwidth the error varies in a range of $\pm 3.2^\circ$ with a maximum value of $\pm 1^\circ$ for Δ_{13-14} and $\pm 2.5^\circ$ for Δ_{23-24}. No tuning has been performed on this prototype.

B. Waveguide 4 × 4 Butler Matrix Based on Resonators

The synthesis and design of a 4 × 4 Butler matrix with filtering is presented in this section. The central frequency is $f_0 = 12.5$ GHz, bandwidth is $B = 500$ MHz, and return loss is 25 dB. According to (19) and (20), the device is expected to exhibit a Chebyshev four-pole transfer function per input–output with a number of $u = 4$ hybrids and $n = 16$ resonators. Initially the g parameters are calculated, and from them the vector of coupling coefficients $M_{h,\mathrm{BPF}}$ is obtained with (21). Thus, the external coupling coefficients are $M_{0,\mathrm{BPF}} = 1.15216$, hybrids coefficients are $K_{u_1} = 0.7360$ and $K_{u_2} = 0.7360$, and the coefficients of the connections between pair of hybrids are $K_{u_1,u_2} = 0.77152$. The denormalized coefficients, calculated with (24), are $Q_e = 18.833$, $k_{u_1} = 0.029441$, $k_{u_2} = 0.029441$, and $k_{u_1,u_2} = 0.030861$. The waveguide configuration for the fundamental hybrid is the configuration shown in Fig. 6(b) for the 2 × 2 coupler with port 2 put on top at the middle of cavity 2 and with a capacitive coupling in order to improve the symmetry in the plane of ports 1 and 2. The fundamental unit-hybrid is implemented in standard WR75 waveguide, and in order to physically connect them, the topology of Fig. 8(a) has been adopted for this solution. Here the dashed lines represent the negative couplings. The topology of Fig. 8(a) produces the transfer function

$$\boldsymbol{T}_{4\times4} = \frac{1}{\sqrt{4}} \begin{bmatrix} 1 & -1 & 1 & 1 \\ -1 & 1 & 1 & 1 \\ 1 & 1 & 1 & -1 \\ 1 & 1 & -1 & 1 \end{bmatrix}. \tag{27}$$

This is still orthogonal, and hence, able to grant the combination and recombination stage required by (1).

The schematic of the dimensions of the single hybrid is shown in Fig. 8(b) with all four hybrids having the same coupling coefficients, and consequently, the same dimensions. Port p_2 is on top of cavity 2 so the capacitive coupling has been filled with grey for better clarity. The other hybrids are mutually coupled with respect to ports q_1 and q_2 only in order to make the design feasible. The coupling k_{u_1,u_2} is performed through a square

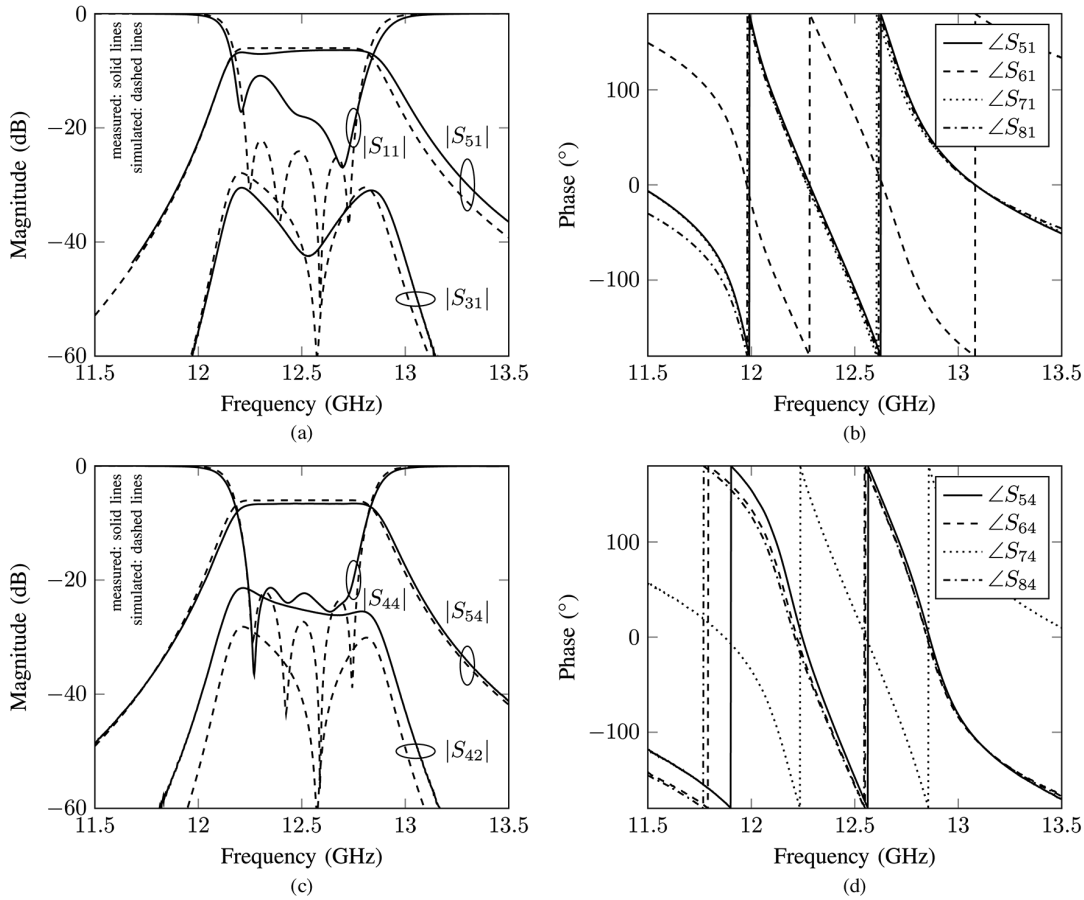

Fig. 9. Measurements of the 4 × 4 Butler matrix with filtering. Additive manufacturing model with input at port 1 magnitude (a) with 180-MHz frequency shift displayed in the measured data and (b) output phases; milling model, input at port 4, (c) magnitude, and (d) output phases.

bend of aperture w_{e3}, hence keeping it inductive. The overall structure is built with two horizontal and two vertical hybrids with the square bends keeping the inductive EM properties of the connecting couplings. Fig. 8(c) shows the 3-D design of the 4 × 4 Butler matrix. With reference to Fig. 8(b), the dimensions in millimeters are $a_1 = 19.242$, $l_1 = 11.906$, $w_{e1} = 9.314$, $w_1 = 8.4468$, $l_3 = 12.2286$, $a_3 = 19.05$, $w_{e3} = 9.341$, $w_2 = 7.9597$, $l_2 = 32.046$, $b_{e2} = 4.0025$, $w_{e2} = 17.3198$, and $a_2 = 18.117$, thickness of iris walls is 1, and 1.5-mm radius is applied to internal corners.

Two realizations of the network have been manufactured, one using additive manufacturing and the other with milling. They are shown in Fig. 8(d). The design and the physical models have been included with identification of input/output ports consistent with Fig. 8(a). Due to the complexity of the 3-D structure, some of the labels are not included in all the figures. The two models are identical, except for the lengths of the external waveguides/interfaces for the version made with milling because it is necessary to allow space for the screws. The additive manufacturing process has the advantage to produce a lighter and monolithic device with no extra pieces that might produce mismatches or misalignments. The price paid is in terms of higher tolerances and roughness intrinsic to this technique, being of 0.1 mm compared with the 20 μm achievable by milling. On the other hand, the 4 × 4 unit manufactured with milling is formed by one main block and four lids. The response of each device is represented by an 8 × 8 complex scattering matrix, thus, in Fig. 9 are just shown as a selection of responses of the two models. The comparison between the measurements (solid lines) and simulations (dashed lines) for the model built with additive manufacturing and milling are shown in Fig. 9(a) and (c). In Fig. 9(b) and (d) are the phase relations for the two models (additive manufacturing and milling, respectively). The input ports are numbered 1, ..., 4 while outputs are 5, ..., 8. Fig. 9(a) is obtained by introducing a frequency offset of 180 MHz in the measured results, as the manufacturing process caused a general shift down in frequency. The offset has been applied in order to easily compare the response with respect to the simulations. The passband S_{51} shows a very good agreement with the theory, as well as the isolation term S_{31}. The return loss is 12 dB in the worst case, which is in line with the tolerances of the manufacturing technique. Even though not all the poles are visible in the return loss, the skirt of S_{51} shows a four-pole Chebyshev characteristic as does the bandwidth and the 6-dB power splitting ratio. The transmission output phases are shown in Fig. 9(b) without the need to apply any frequency offset. The parameters $\angle S_{51}$, $\angle S_{71}$, and $\angle S_{81}$ are in phase while $\angle S_{61}$ is out of phase. This is in agreement with the first row of transfer function matrix (27). The figure also shows the low error in the phase distribution in this device. Fig. 9(c) shows the magnitude response when the input source is applied to port 4 for the model built with a milling technique. The return loss is better than 22 dB, operational bandwidth, isolation, and transmission

are very close to the simulations because of the more accurate building process. The output phases of Fig. 9(d) are consistent with the fourth row of the transfer function matrix (27) as the element $\angle S_{74}$ is out of phase with respect the others. There is a shift in the output phase response with respect to Fig. 9(b): this is due to the different lengths of the external waveguides of the model made with milling. It should be noted that the assembly of the different parts of the milling model leads to small local misalignments and leakages of the EM field that deteriorate the phase stability with respect to the additive manufacturing model. The mismatch appears to be less critical within the operational bandwidth. Both models of Fig. 8(d) have also been manufactured and tested without tuning screws and the measurements included in Fig. 9 correspond to the response without tuning.

The volume occupied by this 4×4 Butler matrix with filtering is 66.2 cm^3. If compared to the example of the conventional ONET shown in Fig. 5(b), it is possible to quantify that the current solution occupies 31.5% less volume with respect to the equivalent Bulter matrix plus four BPFs.

Regarding the 8×8 network of Fig. 4, it can be implemented with a similar structure of Fig. 8(a) repeated twice with four hybrids plus one resonator each connecting the parts.

VII. Conclusions

A new Butler matrix that incorporates BPF functions has been presented in this paper. The basic principles of these networks, as well as their applications in MPAs, have been discussed and some implementation examples for satellite telecommunication applications reported. The solution solves the need to add filtering selectivity at the output of the ONET in order to suppress spurious frequencies generated by the power amplifiers of the MPA. Normally, this is done with extra filters cascaded to the output Butler matrix. In this paper, a new circuit based only on coupled resonators is presented, showing both the power division, phase distribution, and filtering transfer function. Here, the synthesis procedure overcomes the intrinsic problems and limitations of the current techniques for multi-port networks as it is based on the perfect virtual open circuit provided by the 180° hybrid coupler. The advantages in terms of size and mass reduction are a key feature of the present solution. Also, the synthesis presented here is completely general and no assumption has been made over the type of resonator used. Finally, examples of a 2×2 hybrid and a 4×4 Butler matrix derived with the present technique have been shown. Moreover, a 4×4 model has been produced both with additive manufacturing and milling techniques and a discussion on the experimental results has been introduced. Comparison between simulations and measurements show good agreement, both for the magnitude as well as for the output phase.

Acknowledgment

The authors wish to thank Fundación Prodintec for the building of the additive manufacturing Butler matrix, the ESA/ESTEC workshop for making the breadboards with milling, and Aurorasat SL for the support for the Fest3D simulation tool.

References

[1] J. Butler and R. Lowe, "Beam-forming matrix simplifies design of electrically scanned antennas," *Electron. Design*, vol. 9, pp. 170–173, Apr. 1961.

[2] J. Butler, "Multiple beam antenna system employing multiple directional couplers in the leadin," U.S. Patent 3 255 450, Jun. 7, 1966.

[3] J. Allen, "A theoretical limitation on the formation of lossless multiple beams in linear arrays," *IEEE Trans. Antennas Propag.*, vol. AP-9, no. 4, pp. 350–352, Jul. 1961.

[4] J. Shelton and K. S. Kelleher, "Multiple beams from linear arrays," *IRE Trans. Antennas Propag.*, vol. AP-9, no. 2, pp. 154–161, Mar. 1961.

[5] H. Moody, "The systematic design of the Butler matrix," *IEEE Trans. Antennas Propag.*, vol. AP-12, no. 6, pp. 786–788, Nov. 1964.

[6] M. Ueno, "A systematic design formulation for Butler matrix applied FFT algorithm," *IEEE Trans. Antennas Propag.*, vol. AP-29, no. 3, pp. 496–501, May 1981.

[7] D. Pozar, *Microwave Engineering*, 4th ed. New York, NY, USA: Wiley, 2012.

[8] R. Levy and L. Lind, "Synthesis of symmetrical branch-guide directional couplers," *IEEE Trans. Microw. Theory Techn.*, vol. MTT-19, no. 2, pp. 80–89, Feb. 1968.

[9] L. Lind, "Synthesis of asymmetrical branch-guide directional coupler-impedance transformers," *IEEE Trans. Microw. Theory Techn.*, vol. MTT-17, no. 1, pp. 45–48, Jan. 1969.

[10] T. Macnamara, "Simplified design procedures for Butler matrices incorporating 90 ° hybrids or 180 ° hybrids," *Proc. Inst. Elect. Eng.—Microw., Antennas Prop.*, vol. 134, no. 1, pt. H, pp. 50–54, 1987.

[11] W. A. Sandrin, "The Butler matrix transponder," *ComSat Tech. Rev.*, vol. 4, no. 2, pp. 319–345, 1974.

[12] S. Egami and M. Kawai, "An adaptive multiple beam system concept," *IEEE J. Sel. Areas Commun.*, vol. SAC-5, no. 4, pp. 630–636, May 1987.

[13] M. Tanaka and S. Egami, "Reconfigurable multiport amplifiers for in-orbit use," *IEEE Trans. Aerosp. Electron. Syst.*, vol. 42, no. 1, pp. 228–236, Jan. 2006.

[14] P. Angeletti and M. Lisi, "Multiport power amplifiers for flexible satellite antennas and payloads," *Microw. J.*, pp. 96–110, May 2010.

[15] Z. Zhu, X. Huang, and M. Caron, "Ka-band multi-port power amplifier calibration experiment and results," in *2010 2nd Int. Adv. Satellite Space Commun. Conf.*, Jun. 2010, pp. 11–14.

[16] J. Hartmann, J. Habersack, H. Steiner, and M. Lieke, "Advanced communication satellite technologies," presented at the ISRO Space Borne Antennae Technol. Meas. Tech. Workshop, Apr. 2002.

[17] H. Uchida, N. Yoneda, Y. Konishi, and S. Makino, "Bandpass directional couplers with electromagnetically-coupled resonators," in *IEEE MTT-S Int. Microw. Symp. Dig.*, Jun. 2006, pp. 1563–1566.

[18] W.-L. Chang, T.-Y. Huang, T.-M. Shen, B.-C. Chen, and R.-B. Wu, "Design of compact branch-line coupler with coupled resonators," in *Asia–Pacific Microw. Conf.*, Dec. 2007, pp. 1–4.

[19] C.-K. Lin and S.-J. Chung, "A compact filtering 180° hybrid," *IEEE Trans. Microw. Theory Techn.*, vol. 59, no. 12, pp. 3030–3036, Dec. 2011.

[20] C.-F. Chen, T.-Y. Huang, C.-C. Chen, W.-R. Liu, T.-M. Shen, and R.-B. Wu, "A compact filtering rat-race coupler using dual-mode stub-loaded resonators," in *IEEE MTT-S Int Microw. Symp. Dig.*, 2012, pp. 1–3.

[21] U. Rosenberg and S. Amari, "New power distribution (combination) method with frequency selective properties," in *Eur. Microw. Conf.*, Nov. 2012, pp. 1–34, Work Notes W14: Adv. *N*-port Netw. Space Appl.

[22] W.-R. Liu, T.-Y. Huang, C.-F. Chen, T.-M. Shen, and R.-B. Wu, "Design of a 180-degree hybrid with Chebyshev filtering response using coupled resonators," in *IEEE MTT-S Int. Microw. Symp. Dig.*, Jun. 2013, pp. 1–3.

[23] U. Rosenberg, M. Salehi, J. Bornemann, and E. Mehrshahi, "A novel frequency-selective power combiner/divider in single-layer substrate integrated waveguide technology," *IEEE Microw. Wireless Compon. Lett.*, vol. 23, no. 8, pp. 406–408, Aug. 2013.

[24] L.-S. Wu, B. Xia, W.-Y. Yin, and J. Mao, "Collaborative design of a new dual-bandpass 180 ° hybrid coupler," *IEEE Trans. Microw. Theory Techn.*, vol. 61, no. 3, pp. 1053–1066, Mar. 2013.

[25] U. Rosenberg, M. Salehi, S. Amari, and J. Bornemann, "Compact multi-port power combination/distribution with inherent bandpass filter characteristics," *IEEE Trans. Microw. Theory Techn.*, vol. 62, no. 11, pp. 2659–2672, Nov. 2014.

[26] T. Skaik, M. Lancaster, and F. Huang, "Synthesis of multiple output coupled resonator circuits using coupling matrix optimisation," *IET Microw. Antennas Propag.*, vol. 5, no. 9, pp. 1081–1088, 2011.
[27] F. Lin, Q. X. Chu, and S. W. Wong, "Design of dual-band filtering quadrature coupler using $\lambda/2$ and $\lambda/4$ resonators," *IEEE Microw. Wireless Compon. Lett.*, vol. 22, no. 11, pp. 565–567, Nov. 2012.
[28] K. Song, X. Ren, F. Chen, and Y. Fan, "Compact in-phase power divider integrated filtering response using spiral resonator," *IET Microw. Antennas Propag.*, vol. 8, no. 4, pp. 228–234, Mar. 2014.
[29] K. Song, X. Ren, F. Chen, and Y. Fan, "Synthesis and design method of bandpass-response power divider," *Microelectron. J.*, vol. 45, no. 1, pp. 71–77, 2014.
[30] R. Gomez-Garcia, M. Sanchez-Renedo, and J.-M. Munoz-Ferreras, "Microwave filtering power-distribution planar networks," in *IEEE MTT-S Int. Microw. Symp. Dig.*, Jun. 2011, pp. 1–4.
[31] A. Garcia-Lamperez, M. Salazar-Palma, and Y. Zhang, "Analytical synthesis of microwave multiport networks," in *IEEE MTT-S Int. Microw. Symp. Dig.*, Jun. 2004, vol. 2, pp. 455–458.
[32] A. Garcia-Lamperez, S. Llorente-Romano, M. Salazar-Palma, and T. Sarkar, "Efficient electromagnetic optimization of microwave filters and multiplexers using rational models," *IEEE Trans. Microw. Theory Techn.*, vol. 52, no. 2, pp. 508–521, Feb. 2004.
[33] A. Garcia-Lamperez, M. Salazar-Palma, and T. Sarkar, "Compact multiplexer formed by coupled resonators with distributed coupling," in *IEEE Antennas Prop. Soc. Int. Symp.*, Jul. 2005, vol. 1A, pp. 89–92.
[34] F. Loras-Gonzalez, I. Hidalgo-Carpintero, S. Sobrino-Arias, A. Garcia-Lamperez, and M. Salazar-Palma, "A novel ku-band dielectric resonator triplexer based on generalized multiplexer theory," in *IEEE MTT-S Int. Microw. Symp. Dig.*, May 2010, pp. 884–887.
[35] S. Tamiazzo and G. Macchiarella, "Synthesis of duplexers with the common port matched at all frequencies," *IEEE Trans. Microw. Theory Techn.*, vol. 62, no. 1, pp. 46–54, Jan. 2014.
[36] F. Seyfert, M. Olivi, S. Bila, and H. Ezzeddine, "Nevanlinna pick interpolation and multiplexer synthesis," in *Eur. Microw. Conf.*, Nov. 2012, pp. 1–18, Work Notes W14: Adv. N-port Netw. Space Appl.
[37] G. Macchiarella and S. Tamiazzo, "Generation of canonical forms for multiport filtering networks," in *IEEE MTT-S Int. Microw. Symp. Dig.*, Jun. 2014, pp. 1–3.
[38] A. Garcia Lamperez and M. Salazar Palma, "Analytical synthesis of coupling matrices for n-port networks with reactance compensation," in *Eur. Microw. Conf.*, Nov. 2012, pp. 1–34, Work. Notes W14: Adv. N-port Netw. Space Appl..
[39] D. Traina, G. Macchiarella, and T. Sarkar, "Robust formulations of the Cauchy method suitable for microwave duplexers modeling," *IEEE Trans. Microw. Theory Techn.*, vol. 55, no. 5, pp. 974–982, May 2007.
[40] G. Matthaei, E. M. T. Jones, and L. Young, *Microwave Filters, Impedance-Matching Networks, Coupling Structures*. Norwood, MA, USA: Artech House, 1964.
[41] R. J. Cameron, C. M. Kudsia, and R. R. Mansour, *Microwave Filters for Communication Systems*. Hoboken, NJ, uSA: Wiley, 2007.
[42] V. Tornielli di Crestvolant, P. Martin Iglesias, M. Lancaster, and P. Booth, "Multipaction prediction in 180 ° hybrid power divider based on resonant cavities," in *8th MULCOPIM Workshop*, Sep. 2014, pp. 1–8.
[43] U. Rosenberg, "New 'planar' waveguide cavity elliptic function filters," in *25th Eur. Microw. Conf.*, 1995, vol. 1, pp. 524–527.

Vittorio Tornielli di Crestvolant (GSM'14) was born in Reggio Emilia, Italy, in 1986. He received the Laurea Triennale degree in telecommunications engineering from the University of Parma, Parma, Italy, the Laurea Specialistica degree from the Politecnico di Milano, Milan, Italy, in 2010, and is currently working toward the Ph.D. degree at the University of Birmingham, Birmingham, U.K.

He began his doctoral study with the University of Birmingham, U.K., under a networking-partnering initiative with the European Space Agency (ESA) and Airbus Defence and Space. His research interests are the synthesis and design of microwave multi-port distribution networks with inherent filter transfer functions based on all-resonator circuits.

Petronilo Martin Iglesias (M'12) was born in Caceres, Spain, on April 23, 1980. He received the Telecommunication Engineering degree from the Polytechnic University of Madrid, Madrid, Spain, in 2002, and the Master degree from The University of Leeds, Leeds, U.K., in 2012.

He has been working in industry for over ten years as a Microwave Engineer involved with active (high power amplifiers for radar applications) and passive (filters, multiplexers, couplers, etc.) RF hardware design, including two years as a Radar System Engineer with Indra Sistemas, ISDEFE S.A., and Thales Alenia Space Spain. Since Summer 2012, he has been involved with research and development and project support activities related with RF passive hardware developments for the European Space Agency. His research interests are filter synthesis theory, electromagnetic (EM) design and high power prediction, as well as advanced manufacturing techniques for RF passive hardware.

Mr. Iglesias has served as a member of the Technical Program Committee (TPC), IEEE Microwave Theory and Techniques Society (IEEE MTT-S) since 2013.

Michael J. Lancaster (M'91–SM'04) was born in Keighley, Yorkshire, U.K., in 1958. He received the B.Sc. degree in physics and Ph.D. degree from Bath University, Bath, U.K., in 1980 and 1984, respectively. His doctoral research focused on nonlinear underwater acoustics.

Upon leaving Bath University, he joined the Surface Acoustic Wave (SAW) Group, Department of Engineering Science, Oxford University, Oxford, U.K., as a Research Fellow, where his research concerned the design of new novel surface acoustic wave (SAW) devices including filters and filter banks. In 1987, he became a Lecturer with the Department of Electronic and Electrical Engineering, University of Birmingham, Birmingham, U.K., where he lectures on electromagnetic theory and microwave engineering. Shortly after he joined the department, he began the study of the science and applications of high-temperature superconductors, working mainly at microwave frequencies. In 2000, he became Head of the Emerging Device Technology Research Centre, and in 2003, Head of the Department of Electronic, Electrical and Computer Engineering. He has authored or coauthored over 170 papers in refereed journals and 2 books. His current personal research interests include microwave filters and antennas, as well as the high-frequency properties and applications of a number of novel and diverse materials.

Prof. Lancaster is Fellow of the IET and U.K. Institute of Physics. He is a Chartered Engineer and Chartered Physicist. He has served on the IEEE Microwave Theory and Techniques (IEEE MTT-S) International Microwave Symposium (IMS) Technical Committee.